Advances in Materials Research, *Vol. 9, No. 4 (2020) 265-287*
DOI: https://doi.org/10.12989/amr.2020.9.4.265

Predictions of the maximum plate end stresses of imperfect FRP strengthened RC beams: study and analysis

Benferhat Rabia [1,2], Tahar Hassaine Daouadji*[1,2] and Rabahi Abderezak [1,2]

[1] *Laboratory of Geomatics and sustainable development, University of Tiaret, Algeria*
[2] *Department of Civil Engineering, Ibn Khaldoun University of Tiaret, Algeria*

(*Received June 1, 2020, Revised November 12, 2020, Accepted December 14, 2020*)

Abstract. A theoretical method to predict the interfacial stresses in the adhesive layer of reinforced concrete beams strengthened with porous FRP plate is presented in this paper. The effect due to porosity is incorporated utilizing a new modified rule of mixture covering the porosity phases. The adherend shear deformations have been included in the present theoretical analyses by assuming a linear shear stress through the thickness of the adherends. Remarkable effect of the porosity has been noted in the results. Indeed, the resulting interfacial stresses concentrations are considerably smaller than those obtained by other models which neglect the porosity effect. It was found that the interfacial stresses are highly concentrated at the end of the FRP plate, the minimization of the latter can be achieved by using porous FRP plate in particular at the end. It is also shown that the interfacial stresses of the RC beam increase with volume fraction of fibers, but decrease with the thickness of the adhesive layer.

Keywords: interfacial stresses; reinforced concrete beam; porous FRP plate

1. Introduction

Structural elements reinforced with composite plates have been widely utilized in civil, aviation and mechanical building from macro members to micro devices. The utilization of the FRP to strengthen the concrete is an effective solution to increase the general resistance of the concrete structures. Siddika *et al*. (2020) studied the current state-of-the-art on FRP- reinforced RC structures, especially focusing on their performances, failure modes, modelling, challenges and opportunities under various loading scenarios. Mohammed *et al*. (2020) presented a systematic review of current practices for the maintenance of structures utilizing prefabricated composite jackets and discusses the factors affecting structural repair using these jackets. It centers around prefabricated FRP composite jackets and identifies the parameters that influence the effectiveness of this type of repair system. The knowledge of the precise improvement of the bond stresses inside the interface could be significant in the design of RC beams fortified with FRP plate. In this method, the performance of the FRP-concrete interface in giving an effective stress transfer is of crucial importance. Past examinations have demonstrated that interfacial debonding failure will happen at the plate ends because to interfacial stresses. e.g., because of the high solidarity to-weight proportion, high corrosion resistance and excellent fatigue performance, FRP plate are regularly used to retrofit RC

*Corresponding author, Professor, E-mail: daouadjitahar@gmail.com

http://www.techno-press.org/?journal=amr&subpage=5 ISSN: 2234-0912 (Print), 2234-179X (Online)

beams (Zhao and Zhang 2007 and Siddika *et al*. 2019) strengthen metallic and concrete bridges (Ghafoori *et al*. 2018 and Hosseini *et al*. 2019). In these reinforced beams, higher stiffness and strength, or specific functions are intended to be accomplished. Also, by modifying the interface and plate properties, the overall performance of reinforced beams can be enhanced (Hao *et al*. 2020). Zangana *et al*. (2020) investigated the combination of various fibers (Glass, Kevlar, and Zylon) in the creation of trapezoidal corrugated core of the sandwich systems with the mean to achieve the superior performance in specific stiffness/strength, energy absorption, and core damage without increasing structural weight/thickness under low-velocity impact.

As interfacial stresses are difficult to be estimated in tests and laborious work on meshing sensitivity examination is required in numerical simulations (Du *et al*. 2019), the hypothetical solution of interfacial stresses has gotten broad consideration, and the notion of elastic foundation is generally adopted in these analytical investigations. The least complex case is to simplify the adhesive as a shear layer, i.e., the shear-lag model. And in this one-parameter elastic foundation model, the strain distribution is constantly thought to be uniform over the plate thickness, which is reasonable when bending stiffness of the plate is small compared with that of the host beam (De Lorenzis *et al*. 2009). This model was generally utilized in concrete beams reinforced with FRP plates (Triantafillou and Deskovic 1991, Täljsten 1997, Gao *et al*. 2016, Liang *et al*. 2017, Yang *et al*. 2009, Khan *et al*. 2017, Arani *et al*. 2017, Alam *et al*. 2018, Ashour *et al*. 2004 and Esfahani *et al*. 2007).

In their examinations, Shen *et al*. (2001) expected that the longitudinal interfacial stresses change linearly through the adhesive layer thickness. The solution created by Smith and Teng (2001) is famous among all the above solutions but is relevant just for uniformly distributed loads (UDL) and single point loads. Narayanamurthy *et al*. (2011) presented a general analytical solution for the interfacial stresses in plated beams under an arbitrary loading with the shear deformation of the adherends duly considered. Hao *et al*. (2012) developed an improved analytical solution for interfacial stresses that incorporates multiple loading conditions simultaneously, including prestress, mechanical and thermal loads, and the effects of adherend shear deformations and curvature mismatches between the beam and the plate. Daouadji *et al*. (2020) and Tounsi (2006) developed an improved theoretical interfacial stress analysis for simply supported concrete beam bonded with a FRP plate when the adherend shear deformations have been included by assuming a linear shear stress through the thickness of the adherends. Teng and Yao (2007) displayed an experimental investigation on plate end debonding failures in FRP-plated RC beams. Ahmed *et al*. (2011) tested a series of RC beams strengthened with carbon fiber reinforced polymer (CFRP), of which several have been treated this approach, among them (Kaddari *et al*. 2020, Zine *et al*. 2020, Addou *et al*. 2019, Alimirzaei *et al*. 2019, Medani *et al*. 2019, Berghouti *et al*. 2019, Daouadji *et al*. 2016, Rabahi *et al*. 2016, Bourada *et al*. 2019, Benhenni *et al*. 2019a, b, Benferhat *et al*. 2016a, b, Batou *et al*. 2019, Bousahla *et al*. 2020, Belbachir *et al*. 2020, Bourada *et al*. 2020, Shariati *et al*. 2020, Abualnour *et al*. 2019, Belbachir *et al*. 2019, Abderezak *et al*. 2020, Tounsi *et al*. 2008, Daouadji and Benferhat 2016, Sahla *et al*. 2019, Draiche *et al*. 2019, Matouk *et al*. 2020 and Chikr *et al*. 2020). Daouadji *et al*. (2016) presented an interfacial stress analysis for simply supported concrete beam bonded with a functionally graded material FGM plate. Hadji *et al*. (2016) a presented a theoretical method to predict the interfacial stresses in the adhesive layer of reinforced concrete beams strengthened with externally bonded carbon fiber-reinforced polymer (CFRP). Hojatkashani and Kabir (2012) presented an experimental examination to study interfacial stresses developed at the junction zones between carbon fiber reinforced plastic (CFRP) fabrics and tensile concrete portion in CFRP retrofitted RC beams. Abderezak *et al*. (2017) presented a simple closed-form solution to calculate the interfacial shear and normal stresses of retrofitted concrete beam strengthened with thin composite plate under mechanical loads including the creep and shrinkage effect. Chedad *et al*. (2017) developed an improved theoretical solution for interfacial stress analysis for simply supported concrete beam bonded with a sandwich FGM plate, thing that was analyzed by (Khiloun *et al*. 2020, Chedad *et al*. 2018, Chergui *et al*. 2019, Daouadji *et al*. 2016, Rahmani *et al*. 2020, Abderezak *et al*. 2018, Abdelhak *et al*. 2016, Belkacem *et al*. 2018, Rabhi *et al*. 2020, and Adim and Daouadji 2016, Refrafi *et al*. 2020, Benhenni *et al*. 2019, Tounsi *et al*. 2020, Hussain *et al*. 2020, Boussoula *et al*. 2020, Bensattalah *et al*. 2016, Al-Furjan *et al*. 2020, Rabahi *et al*. 2019, Benferhat *et al*. 2016, Balubaid *et al*. 2019, Hamrat *et al*. 2020, Daouadji 2013, Chikr *et al*. 2019, Bouakaz *et al*. 2014, Boutaleb *et al*. 2019 and Karami *et al*. 2019). In contrast, more investigations were completed to compute the interfacial stresses of RC beam by utilizing finite element method (FEM). Remarkable works are due to Teng *et al*. (2002) where they developed a careful finite element investigation into interfacial stresses in reinforced concrete ŽRC. beams strengthened with a bonded soffit plate, with the aims of assessing the accuracy of existing approximate closed-form analytical solutions based on simplifying assumptions and highlighting aspects which are omitted by them. However, in FRP composite, micro voids or porosities can occur within the matrix of the reinforcement plate during the process of fabrication. Therefore, it is important to take into account the porosity effect in the study of the interfacial stresses of the RC beam strengthened with FRP plate (Tayeb and Daouadji 2020, Hadj *et al*. 2019 and Daouadji 2016).

In the present work, we focus our attention on the effect of porosity in the interfacial stresses for simply supported RC beam bonded with a porous FRP composite to the tension face. A new modified rule of mixture which takes into account the effect of porosity in FRP reinforcing plates was proposed in this work. This porosity can occur in the matrix of FRP plates during their manufacture. To the authors' knowledge, no researcher has given much attention to the effect of porosity on the interfacial stresses of a concrete beam reinforced with a composite plate. The solution is generic and applicable to beams and plates made of any structural materials within the linear elastic range, in common with almost all previous studies. Numerical comparison of the new solution with one of the existing solutions for three loading cases illustrate the accuracy and applicability of the new analytical solution. A parametric study is performed to show the effect of the porosity and the geometric parameters on the interfacial stresses.

2. Theoretical analysis and solutions procedure

2.1 Presentation of the rehabilitation technique and solution method

In order to give the lost rigidity to the beams in bending reinforced concrete, we used composite plates bonded externally on the tensed surfaces. Among these composite materials, fiber reinforced polymers (FRP) are widely used due to their unmatched characteristics. The transfer of stresses from concrete to FRP reinforcements is at the heart of the strengthening effect of concrete structures reinforced with FRP (Daouadji 2017, Benhenni *et al*. 2018, Rabia *et al*. 2018 and Bensattalah *et al*. 2018). Indeed, stresses are likely to cause undesirable premature and fragile failure. In the reinforcement of reinforced concrete beams with FRP strips, different failure modes have been observed. Generally, there are six distinct failure modes (Fig. 1), as described below.

Fig. 1 Failure modes of FRP strengthened RC beams

- *Compression failure before yielding of steel:* the concrete crushes in compression (i.e., the strain in the concrete exceeds the ultimate value of 0.0035) before yielding of reinforcing steel and fracture of FRP strips;
- *Compression failure after yielding of steel:* the reinforcing steel yields due to tensile flexure. This is followed by crushing of the concrete in the compression zone, before the tensile rupture of the FRP strips;
- *Rupture of FRP strips:* the FRP strips rupture at the ultimate strain following the yielding of reinforcing steel rebar in tension;
- *Shear failure:* the shear cracks extend from the vicinity of the support to the loading point, when the shear capacity of the beam is exceeded;
- *Delamination of FRP strips:* delamination of CFRP strip occurs rather catastrophically in an unstable manner, with a thin layer of concrete residue attached to the delaminated FRP sheets. The crack initiates from the end of FRP strips or the bottom of a flexural or shear/flexural crack in the concrete member; (vi) Concrete cover separation: after crack initiation at the CFRP strip end, the CFRP strip is gradually peeled off with lumps of concrete detached from the longitudinal steel rebar.

The present study is devoted to understand the mechanism of debonding failure mode and develop sound design rules. This brittle mode of failure is a result of the high shear and vertical normal (peeling) stress concentrations arising at the edges of the bonded imperfect FRP strip. Hence, this limited area in the close vicinity of the bonded strip edge, subjected to high peeling and interfacial shear stresses, proves to be among the most critical parts of the strengthened beams. This is the purpose of our present study.

2.2 Assumptions of the present solution

The present analysis takes into consideration the transverse shear stress and strain in the beam and the plate but ignores the transverse normal stress in them. One of the analytical approach proposed by Daouadji *et al*. (2019) for concrete beam strengthened with a bonded imperfect FRP Plate (Fig. 2) was used in order to compare it with a finite element analysis. The analytical approach (Daouadji *et al*. 2019) is based on the following assumptions.

- Elastic stress strain relationship for concrete, composite and adhesive;
- There is a perfect bond between the imperfect composite plate and the RC beam;
- The adhesive is assumed to only play a role in transferring the stresses from the concrete to the porous composite plate reinforcement;
- The stresses in the adhesive layer do not change through the direction of the thickness.

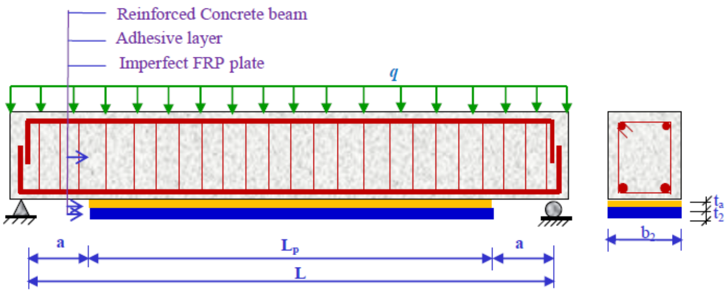

Fig. 2 Simply supported RC beam strengthened with bonded imperfect FRP plate

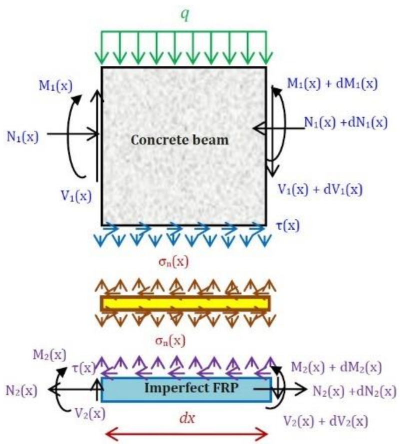

Fig. 3 Forces in differential element of the plated beam

Since the porous FRP laminate is an orthotropic material, its material properties vary from layer to layer. In analytical study (Daouadji *et al*. 2019 and Rabia *et al*. 2019a, b), the laminate theory is used to determine the stress and strain behaviours of the externally bonded imperfect composite plate in order to investigate the whole mechanical performance of the composite – strengthened structure. The laminate theory is used to estimate the strain of the symmetrical porous composite plate.

The linear constitutive relations of a FG plate can be written as

$$\begin{Bmatrix} \sigma_x \\ \sigma_y \\ \sigma_{xy} \\ \sigma_{yz} \\ \sigma_{xz} \end{Bmatrix} = \begin{bmatrix} Q_{11} & Q_{12} & 0 & 0 & 0 \\ Q_{12} & Q_{22} & 0 & 0 & 0 \\ 0 & 0 & Q_{66} & 0 & 0 \\ 0 & 0 & 0 & Q_{44} & 0 \\ 0 & 0 & 0 & 0 & Q_{55} \end{bmatrix} \begin{Bmatrix} \varepsilon_x \\ \varepsilon_y \\ \gamma_{xy} \\ \gamma_{yz} \\ \gamma_{xz} \end{Bmatrix} \tag{1}$$

Where Q_{ij} are the rigidities of the layer considered

$$Q_{11} = \frac{E_1}{1 - \nu_{12}\nu_{21}} \tag{2a}$$

$$Q_{12} = \frac{\nu_{12}E_2}{1 - \nu_{12}\nu_{21}} \tag{2b}$$

$$Q_{22} = \frac{E_2}{1 - \nu_{12}\nu_{21}} \tag{2c}$$

$$Q_{66} = G_{12} \tag{2d}$$

$$Q_{44} = G_{23} \tag{2e}$$

$$Q_{55} = G_{13} \tag{2f}$$

where (σ_x, σ_y, τ_{xy}, τ_{yz}, τ_{yx}) and (ε_x, ε_y, γ_{xy}, γ_{yz}, γ_{yx}) are the stress and strain components, respectively , and A_{ij}, D_{ij} are the plate stiffness, of the laminate are given as follows

Extensional matrix

$$A_{ij} = \sum_{kl=1}^{NL} \left(\overline{Q_{ij}}\right)_{kl} (z_{kl} - z_{kl-1}) \tag{3}$$

Extensional-bending coupled matrix

$$B_{ij} = \frac{1}{2} \sum_{kl=1}^{NL} \left(\overline{Q_{ij}}\right)_{kl} \left(z_{kl}^2 - z_{kl-1}^2\right) \tag{4}$$

Flexural matrix

$$D_{ij} = \frac{1}{3}\sum_{kl=1}^{NL} \left(\overline{Q_{ij}}\right)_{kl} \left(z_{kl}^3 - z_{kl-1}^3\right) \tag{5}$$

where $A_{11}^{'}$, $D_{11}^{'}$ are defined as

$$A_{11}^{'} = \frac{A_{22}}{A_{11}A_{22} - A_{12}^2} \tag{6}$$

$$D_{11}^{'} = \frac{D_{22}}{D_{11}D_{22} - D_{12}^2} \tag{7}$$

where the $\left(\overline{Q_{ij}}\right)_{kl}$ are the transformed stiffness's of the layer number "k_l" of the laminate and can be estimated by using the off-axis orthotropic ply theory.

In terms of micromechanical model of laminate, and taking into account the porosity of the composite (presence of pores in the polymer matrix); the properties of materials can be written

$$E_1 = E_f + \frac{v_m(1-\alpha)}{v_c}(E_m - E_f) = E_f + \mu_m(1-\alpha)(E_m - E_f) \tag{8}$$

$$\frac{1}{E_2} = \frac{\mu_f}{E_f} + \frac{\dfrac{v_m(1-\alpha)}{v_f + v_m(1-\alpha)}}{E_m} - \mu_f \frac{v_m(1-\alpha)}{v_f + v_m(1-\alpha)} \frac{v_f^2\left(\dfrac{E_m}{E_f}\right) + v_m(1-\alpha)^2\left(\dfrac{E_f}{E_m}\right) - 2v_f v_m(1-\alpha)}{\mu_f E_f + \dfrac{v_m(1-\alpha)}{v_f + v_m(1-\alpha)} E_m} \tag{9}$$

$$\frac{1}{G_{12}} = \frac{\mu_f}{G_f} + \frac{\dfrac{v_m(1-\alpha)}{v_f + v_m(1-\alpha)}}{G_m} \tag{10}$$

$$G_{13} = G_{23} = \frac{E_2}{2\,(1 + \upsilon_{12})} \tag{11}$$

$$v_{12} = \mu_f v_f + \frac{v_m(1-\alpha)}{v_f + v_m(1-\alpha)} v_m \tag{12}$$

$$\frac{\upsilon_{12}}{E_1} = \frac{\upsilon_{21}}{E_2} \quad \Rightarrow \quad \nu_{21} = \mu_f v_f + \frac{v_m(1-\alpha)}{v_f + v_m(1-\alpha)} v_m \frac{E_2}{E_1} \tag{13}$$

E_f, G_f and ν_f are the Young's modulus, shear modulus and Poisson's ratio, respectively, of the FRP laminate, and E_m, G_m and ν_m are the corresponding properties for the matrix.

In the above equation, μ_f and μ_m are fiber and matrix volume fractions and are related by

$$\mu_f + \mu_m = 1 \tag{14}$$

with

$$\mu_f = \frac{v_f}{v_c} \qquad \text{and} \qquad \mu_m = \frac{v_m}{v_c} \tag{15}$$

2.3 Shear stress distribution along the FRP – concrete interface

The governing differential equation for the interfacial shear stress is expressed as Rabia *et al.* (2019a)

$$\frac{d^2\tau(x)}{dx^2} - \frac{\left(A'_{11} + \frac{b_2}{E_1A_1} + \frac{\left(y_1 + \frac{t_2}{2}\right)\left(y_1 + t_a + \frac{t_2}{2}\right)}{E_1I_1D'_{11} + b_2} b_2D'_{11}\right)}{\frac{1}{\frac{t_a}{G_a} + \frac{t_1}{4G_1}}}\tau(x) + \frac{\left(\frac{(y_1 + t_2/2)}{E_1I_1D'_{11} + b_2}D'_{11}\right)}{\frac{1}{\frac{t_a}{G_a} + \frac{t_1}{4G_1}}}V_T(x) = 0 \tag{16}$$

For simplicity, the general solutions presented below are limited to loading which is either concentrated or uniformly distributed over part or the whole span of the beam, or both. For such loading, $d^2V_T(x)/dx^2 = 0$, and the general solution to Eq. (16) is given by

$$\tau(x) = B_1\cosh(\phi x) + B_2\sinh(\phi x) + \frac{\frac{1}{\frac{t_a}{G_a} + \frac{t_1}{4G_1}}}{\phi^2}\left(\frac{y_1 + \frac{t_2}{2}}{E_1I_1D'_{11} + b_2}D'_{11}\right)V_T(x) \tag{17}$$

Where

$$\phi = \left[\frac{\left(A'_{11} + \frac{b_2}{E_1A_1} + \frac{(y_1 + t_2/2)(y_1 + t_a + t_2/2)}{E_1I_1D'_{11} + b_2}b_2D'_{11}\right)}{\frac{1}{\frac{t_a}{G_a} + \frac{t_1}{4G_1}}}\right]^{\frac{1}{2}} \tag{18}$$

And B_1 and B_2 are constant coefficients determined from the boundary conditions. In the present study, a simply supported beam has been investigated which is subjected to a uniformly distributed load (Fig. 3). The interfacial shear stress for this uniformly distributed load at any point is written as (Rabia *et al.* 2019a)

$$\tau(x) = \left[\frac{0{,}5.\,ay_1}{E_1I_1\left(\frac{t_a}{G_a} + \frac{t_1}{4G_1}\right)}(l - a) - \frac{1}{\left(\frac{t_a}{G_a} + \frac{t_1}{4G_1}\right)\phi^2}\left(\frac{y_1 + 0{,}5t_2}{E_1I_1D'_{11} + b_2}D'_{11}\right)\right]\frac{qe^{-\lambda x}}{\phi} + \frac{1}{\phi^2\left(\frac{t_a}{G_a} + \frac{t_1}{4G_1}\right)}\left(\frac{y_1 + 0{,}5t_2}{E_1I_1D'_{11} + b_2}D'_{11}\right)q\left(\frac{l}{2} - a - x\right) \qquad 0 \le x \le L_P \tag{19}$$

Where q is the uniformly distributed load and x; a; l and l_p are defined in Fig. 2.

2.4 Normal stress distribution along the FRP – concrete interface

The following governing differential equation for the interfacial normal stress (Rabia *et al*. 2019a)

$$\frac{d^4\sigma_n(x)}{dx^4} + K_n\left(D_{11}^{'} + \frac{b_2}{E_1 I_1}\right)\sigma_n(x) - K_n\left(D_{11}^{'}\frac{t_2}{2} - \frac{y_1 b_2}{E_1 I_1}\right)\frac{d\tau(x)}{dx} + \frac{qK_n}{E_1 I_1} = 0 \tag{20}$$

The general solution to this fourth–order differential equation is

$$\begin{aligned}\sigma_n(x) &= e^{-\beta x}[B_3 \cos(\eta x) + B_4 \sin(\eta x)] \\ &\quad + e^{\beta x}[B_5 \cos(\eta x) + B_6 \sin(\eta x)] - \zeta_1 \frac{d\tau(x)}{dx} - \frac{q}{D_{11}^{'} E_1 I_1 + b_2}\end{aligned} \tag{22}$$

For large values of x it is assumed that the normal stress approaches zero and, as a result, $B_5 = B_6 = 0$. The general solution therefore becomes

Where

$$\sigma_n(x) = e^{-\beta x}[B_3 \cos(\eta x) + B_4 \sin(\eta x)] - \zeta_1 \frac{d\tau(x)}{dx} - \frac{q}{D_{11}^{'} E_1 I_1 + b_2} \tag{23}$$

$$\begin{aligned}\eta &= \sqrt[4]{\frac{K_n}{4}\left(D_{11}^{'} + \frac{b_2}{E_1 I_1}\right)} \\ \zeta_1 &= \left(\frac{y_1 b_2 - D_{11}^{'} E_1 I_1 t_2/2}{D_{11}^{'} E_1 I_1 + b_2}\right)\end{aligned} \tag{24}$$

As is described by Benferhat *et al*. (2019a), the constants B_3 and B_4 in Eq. (22) are determined using the appropriate boundary conditions and they are written as follows

$$B_3 = \frac{K_n}{2\eta^3 E_1 I_1}[V_T(0) + \eta M_T(0)] - \frac{\zeta_2}{2\eta^3}\tau(0) + \frac{\zeta_1}{2\eta^3}\left(\frac{d^4\tau(0)}{dx^4} + \eta\frac{d^3\tau(0)}{dx^3}\right) \tag{25}$$

$$B_4 = -\frac{K_n}{2\eta^2 E_1 I_1} M_T(0) - \frac{\zeta_1}{2\eta^2}\frac{d^3\tau(0)}{dx^3} \tag{26}$$

$$\zeta_2 = b_2 K_n\left(\frac{y_1}{E_1 I_1} - \frac{D_{11}^{'} t_2}{2b_2}\right) \tag{27}$$

The above expressions for the constants B_3 and B_4 has been left in terms of the bending moment $M_T(0)$ and shear force $V_T(0)$ at the end of the soffit plate. With the constants B_3 and B_4 determined, the interfacial normal stress can then be found using Eq. (22).

3. Results: Discussion and analysis

In this section, numerical examples and parametric investigations are displayed for a simply supported FRP-plated concrete beam containing porosity. Results of the interfacial stress of RC beam reinforced with perfect FRP plate are verified by comparison with those given in the literature. Then the mechanical and geometrical properties are varied in order to show their effect on the stress distribution along the externally bonded composite plate-concrete interface. For numerical applications, the mechanical and geometrical characteristics given in Table 1 are equivalent to those utilized by Tounsi (2006).

Table 1 Dimensions and material properties

Concrete	b_1 = 155 mm	t_1 = 225 mm	E_1 = 31,000 MPa
Steel	b_2 = 125 mm	t_2 = 6 mm	E_2 = 200,000 MPa
Adhesive	b_a = 125 mm	t_a = 1.5 mm	E_a = 280 MPa G_a = 108 MPa

Table 2 Porosity effect on the interfacial stresses of a RC beam reinforced and subjected to uniformly distributed loading

Theory	Porosity α	GFRP		CFRP		Steel	
		$\tau(x)$ (MPa)	$\sigma_n(x)$ (MPa)	$\tau(x)$ (MPa)	$\sigma_n(x)$ (MPa)	$\tau(x)$ (MPa)	$\sigma_n(x)$ (MPa)
Tounsi (2006)	α = 0	1.0885	0.826	1.791	1.078	2.120	1.175
Present	α = 0	1.0856	0.82607	1.7914	1.0779	2.1204	1.1751
	α = 0.1	1.0634	0.81675	1.7796	1.0743	2.1189	1.1746
	α = 0.2	1.0407	0.80702	1.7678	1.0707	2.1176	1.1744

Table 3 Porosity effect on the interfacial stresses of a RC beam reinforced and subjected to mid and two point loads

Load	Theory	Porosity α	$\tau(x)$ (MPa)	$\sigma_n(x)$ (MPa)
Mid-point load	Tounsi (2006)	α = 0	2.2385	1.3345
	Smith and Teng (2001)	α = 0	4.3103	2.3644
	Present	α = 0	2.2385	1.3345
		α = 0.1	2.2235	1.3297
		α = 0.2	2.2083	1.3251
Two point load	Tounsi (2006)	α = 0	2.2348	1.2972
	Smith and Teng (2001)	α = 0	4.7208	2.5330
	Present	α = 0	2.2348	1.2972
		α = 0.1	2.2220	1.2939
		α = 0.2	2.2090	1.2907

Tables 2 and 3 presents a comparison of the results of normal and shear stresses of a reinforced RC beam by external bonding of the composite plates for different types of loading. The porosity effect is taken into account in these tables. From these results it can be seen that the interfacial stress become lower when the reinforcing plate contains porosity. It may also be noted that the interfacial stress become larger as the reinforcing plate is made of steel.

Table 4 shows the effect ratio t_2/t_a on the normal and shear stresses of a reinforced concrete beam. The beam is bending reinforced and subjected to uniformly distributed loading. The volume fraction of porosity is considered equal to (0, 0.1 and 0.2). The reinforcement plate is considered in GFRP, CRFP and steel. It is clear that increasing the ratio t_2/t_a increases the interfacial stress whatever the type of reinforcement plate.

Table 4 Effect of the ratio t2/ta on the interfacial stresses of RC beam and subjected to uniformly distributed loading

t_2/t_a	Porosity α	GFRP		CFRP		Steel	
		$\tau(x)$ (MPa)	$\sigma_n(x)$ (MPa)	$\tau(x)$ (MPa)	$\sigma_n(x)$ (MPa)	$\tau(x)$ (MPa)	$\sigma_n(x)$ (MPa)
1	$\alpha = 0$	0.76554	0.48644	1.2928	0.64588	1.5474	0.71080
	$\alpha = 0.1$	0.74955	0.48083	1.2835	0.64350	1.5462	0.71048
	$\alpha = 0.2$	0.73327	0.47508	1.2743	0.64097	1.5452	0.71026
1.5	$\alpha = 0$	0.94034	0.66347	1.5706	0.87387	1.8693	0.95723
	$\alpha = 0.1$	0.92091	0.65581	1.5599	0.87088	1.8680	0.95679
	$\alpha = 0.2$	0.90099	0.64802	1.5491	0.86768	1.8668	0.95656
2	$\alpha = 0$	1.0856	0.82607	1.7914	1.0779	2.1204	1.1751
	$\alpha = 0.1$	1.0634	0.81675	1.7796	1.0743	2.1189	1.1746
	$\alpha = 0.2$	1.0407	0.80702	1.7678	1.0707	2.1176	1.1744

Table 5 Effect of the ratio t1/b1 on the interfacial stresses of RC beam and subjected to a uniformly distributed loading

t_1/b_1	Porosity α	GFRP		CFRP		Steel	
		$\tau(x)$ (MPa)	$\sigma_n(x)$ (MPa)	$\tau(x)$ (MPa)	$\sigma_n(x)$ (MPa)	$\tau(x)$ (MPa)	$\sigma_n(x)$ (MPa)
1	$\alpha = 0$	1.9666	1.2468	3.2394	1.6208	5.0641	2.8310
	$\alpha = 0.1$	1.9267	1.2329	3.2178	1.6154	5.0612	2.8306
	$\alpha = 0.2$	1.8861	1.2188	3.1961	1.6098	5.0587	2.8295
1.5	$\alpha = 0$	1.0856	0.82607	1.7914	1.0779	2.1204	1.1751
	$\alpha = 0.1$	1.0634	0.81675	1.7796	1.0743	2.1189	1.1746
	$\alpha = 0.2$	1.0407	0.80702	1.7678	1.0707	2.1176	1.1744
2	$\alpha = 0$	0.55681	0.42401	0.94124	0.56492	1.1252	0.62127
	$\alpha = 0.1$	0.54501	0.41893	0.93466	0.56281	1.1243	0.62100
	$\alpha = 0.2$	0.53303	0.41376	0.92795	0.56065	1.1236	0.62083

Table 6 Interfacial stresses of RC beam strengthened with FRP plate for different E_1 values

E_1 (MPa)	Porosity α	GFRP		CFRP		Steel	
		$\tau(x)$ (MPa)	$\sigma_n(x)$ (MPa)	$\tau(x)$ (MPa)	$\sigma_n(x)$ (MPa)	$\tau(x)$ (MPa)	$\sigma_n(x)$ (MPa)
20000	$\alpha = 0$	1.3727	1.0600	2.2069	1.3482	2.5650	1.4450
	$\alpha = 0.1$	1.3454	1.0487	2.1936	1.3444	2.5634	1.4447
	$\alpha = 0.2$	1.3173	1.0366	2.1802	1.3407	2.5620	1.4444
30000	$\alpha = 0$	1.0856	0.82607	1.7914	1.0779	2.1204	1.1751
	$\alpha = 0.1$	1.0634	0.81675	1.7796	1.0743	2.1189	1.1746
	$\alpha = 0.2$	1.0407	0.80702	0.94124	1.0707	2.1176	1.1744
50000	$\alpha = 0$	0.78806	0.58914	1.3289	0.78655	1.6036	0.87343
	$\alpha = 0.1$	0.77158	0.58208	1.3195	0.78357	1.6025	0.87315
	$\alpha = 0.2$	0.75473	0.57490	1.3101	0.78050	1.6013	0.87283

The effect of beam geometry (ratio t_1/b_1) on normal and shear stresses for a reinforced concrete beam is shown in Table 5. The shape of the beam is considered square and rectangular. The thickness of the adhesive is taken equal to (t_a = 2 mm). From these results, it can be concluded that the interfacial stress become more important when the concrete shape of the beam is square.

The effect of the Young's modulus of the beam on the normal and shear stresses of a bending-reinforced beam is shown in Table 6. Young's modulus of the beam is equal (20000, 30000 and 50000 MPa). The thickness of the reinforcing plate is taken as (t_2 = 4 mm). From these results, it can be concluded that the interfacial stress become weaker as the Young's modulus of the beam increases.

Table 7 shows the effect of the Young's modulus of the adhesive on the normal and shear stresses of a reinforced concrete beam reinforced by external bonding of the composite plates. The Young's modulus of the adhesive is taken equal (3000, 4000 and 5000 MPa). The thickness of the adhesive is taken equal to (t_a = 2), while the thickness of the reinforcement plate is taken equal to (t_2 = 4 mm).

Table 7 Interfacial stresses of RC beam strengthened with FRP plate for different E_a values

E_a (MPa)	Porosity α	GFRP		CFRP		Steel	
		$\tau(x)$ (MPa)	$\sigma_n(x)$ (MPa)	$\tau(x)$ (MPa)	$\sigma_n(x)$ (MPa)	$\tau(x)$ (MPa)	$\sigma_n(x)$ (MPa)
3000	$\alpha = 0$	1.0856	0.82607	1.7914	1.0779	2.1204	1.1751
	$\alpha = 0.1$	1.0634	0.81675	1.7796	1.0743	2.1189	1.1746
	$\alpha = 0.2$	1.0407	0.80702	0.94124	1.0707	2.1176	1.1744
4000	$\alpha = 0$	1.1085	0.91032	1.8274	1.1866	2.1631	1.2938
	$\alpha = 0.1$	1.0859	0.90016	1.8154	1.1827	2.1612	1.2933
	$\alpha = 0.2$	1.0626	0.88934	1.8032	1.1788	2.1593	1.2926
5000	$\alpha = 0$	1.1229	0.97887	1.8500	1.2748	2.1903	1.3902
	$\alpha = 0.1$	1.1000	0.96787	1.8379	1.2708	2.1880	1.3896
	$\alpha = 0.2$	1.0765	0.95627	1.8256	1.2665	2.1857	1.3890

Table 8 Influence of the distance from the support to the end of the plate on the interfacial stresses of RC beam strengthened with FRP plate

a	Porosity α	GFRP		CFRP		Steel	
		$\tau(x)$ (MPa)	$\sigma_n(x)$ (MPa)	$\tau(x)$ (MPa)	$\sigma_n(x)$ (MPa)	$\tau(x)$ (MPa)	$\sigma_n(x)$ (MPa)
50	$\alpha = 0$	0.32110	0.24646	0.62157	0.37406	0.77176	0.42629
	$\alpha = 0.1$	0.31261	0.24225	0.61610	0.37203	0.77103	0.42604
	$\alpha = 0.2$	0.30395	0.23787	0.61066	0.37000	0.77039	0.42586
100	$\alpha = 0$	0.48594	0.37144	0.87415	0.52604	1.0631	0.58805
	$\alpha = 0.1$	0.47446	0.36611	0.86730	0.52366	1.0622	0.58778
	$\alpha = 0.2$	0.46278	0.36058	0.86048	0.52126	1.0614	0.58756
200	$\alpha = 0$	0.79770	0.60778	1.3514	0.81323	1.6133	0.89353
	$\alpha = 0.1$	0.78068	0.60044	1.3420	0.81022	1.6121	0.89320
	$\alpha = 0.2$	0.76322	0.59266	1.3325	0.80716	1.6111	0.89297

From these results, it can be seen that the interfacial stress increase with increasing Young's modulus of the adhesive.

Table 8 shows the effect of the distance of the support at the end of the plate (a) on the normal and shear stresses of a RC beam reinforced in the bending. The distance of the support at the end of the plate is equal (50, 100 and 200 mm). The thickness of the reinforcing plate is taken equal to (t_2 = 4 mm). It may be noted that the interfacial stress become more important when the distance of the support at the end of the plate increases.

Figs. 4(a) and (b) show the effect of porosity in the reinforcing plate on the normal stress of a RC beam reinforced by external bonding a porous composite plate. The composite reinforcement plate is considered in Kevlar and Glass fiber, respectively. The thickness of the adhesive is taken equal to (t_a = 2 mm). From these figures, it can be seen that the porosity effect on the normal stress increases as the thickness of the reinforcement plate increases.

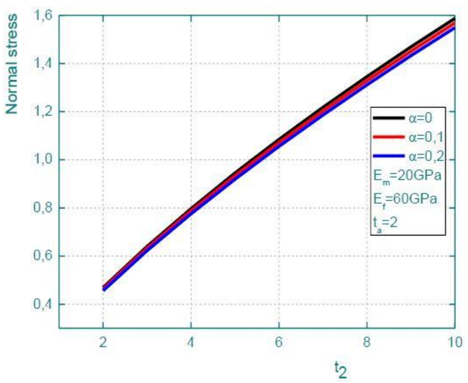

(a) Kevlar FRP

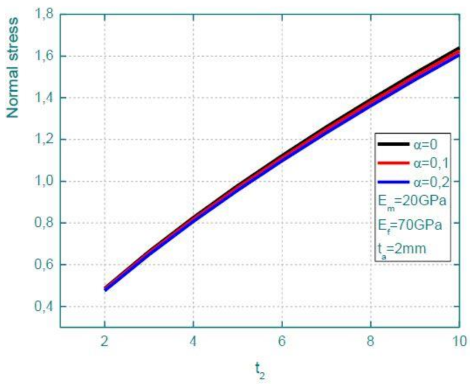

(b) Glass FRP

Fig. 4 Porosity effect as function of plate thickness on normal stress of RC beam strengthened with Kevlar and Glass FRP plate

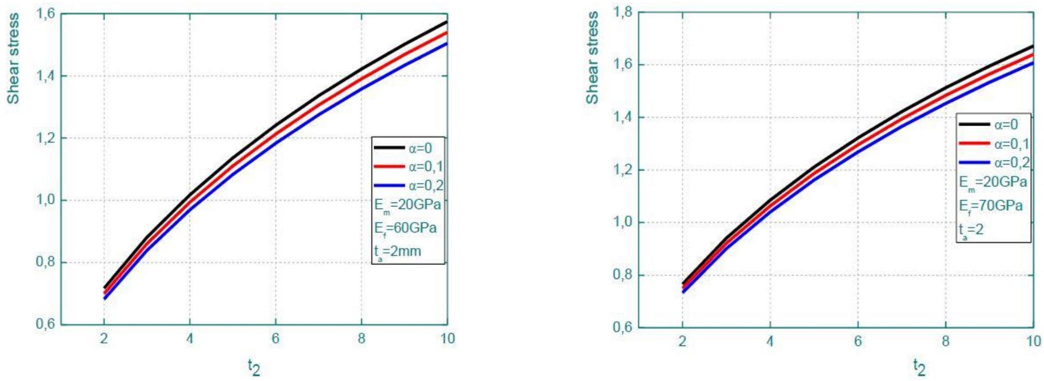

(a) Kevlar FRP (b) Glass FRP

Fig. 5 Porosity effect as function of plate thickness on shear stress of RC beam strengthened with Kevlar and Glass FRP plate

Figs. 5(a) and (b) show the influence of the volume fraction of porosity as a function of the thickness of the reinforcement plate on the shear stress of a RC beam subjected to uniformly distributed load and reinforced in bending by a Kevlar and GFRP plate, respectively. It should be noted that the volume fraction of porosity reduces the shear stresses. It can also be seen that the shear stresses become greater as the reinforcement plate becomes thicker.

The porosity effect and thickness of the adhesive on the normal stress of a RC beam reinforced with a Kevlar and GFRP plate is shown in Figs. 6(a) and (b), respectively. The thickness of the reinforcement plate is taken equal to (t_2 = 2 mm). The load is considered uniformly distributed. It can be seen from these figures that the normal stress becomes lower as the thickness of the adhesive increases. The variation in shear stress versus adhesive thickness of a RC beam reinforced with a Kevlar and GFRP porous composite plate is shown in Fig. 7(a) and (b), respectively. The volume fraction of the fibers is considered equal to 0.6. It can be seen that the volume fraction of porosity has more effect on shear stresses than normal stresses.

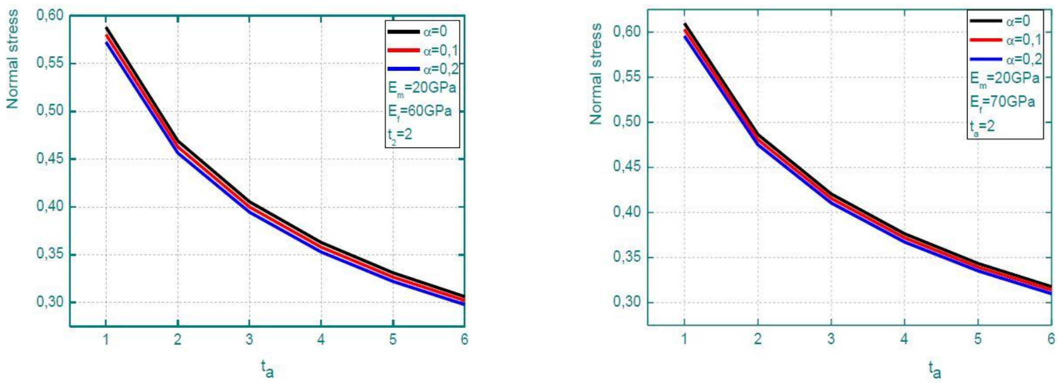

(a) Kevlar FRP (b) Glass FRP

Fig. 6 Porosity effect as function of adhesive thickness on normal stress of RC beam strengthened with Kevlar and Glass FRP plate

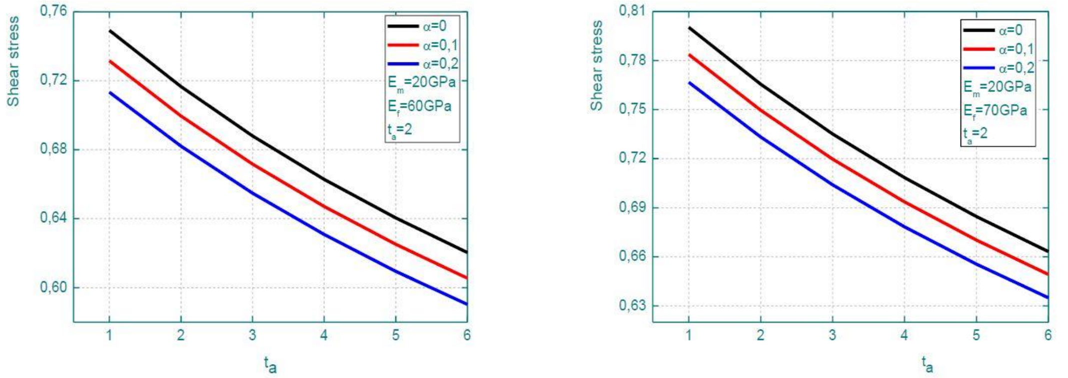

(a) Kevlar FRP (b) Glass FRP

Fig. 7 Porosity effect as function of adhesive thickness on shear stress of RC beam strengthened with Kevlar and Glass FRP plate

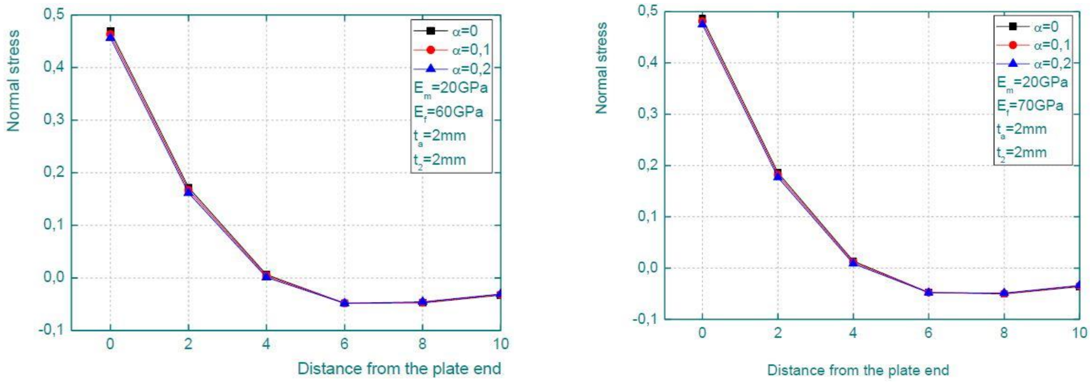

(a) Kevlar FRP (b) Glass FRP

Fig. 8 Porosity effect as function of distance from the plate end on normal stress of RC beam strengthened with Kevlar and Glass FRP plate

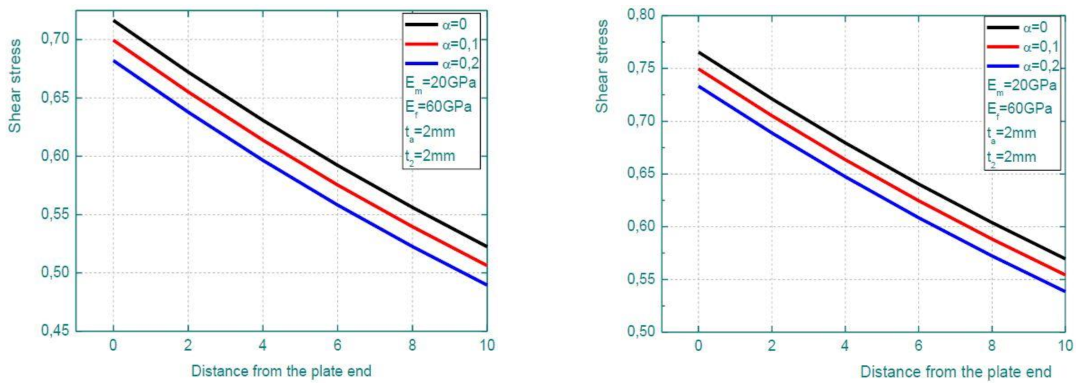

(a) Kevlar FRP (b) Glass FRP

Fig. 9 Porosity effect as function of distance from the plate end on shear stress of RC beam strengthened with Kevlar and Glass FRP plate

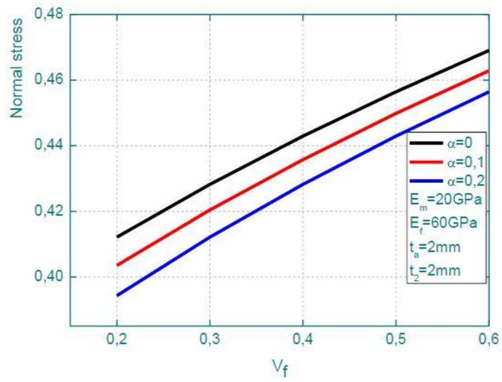

(a) Kevlar FRP

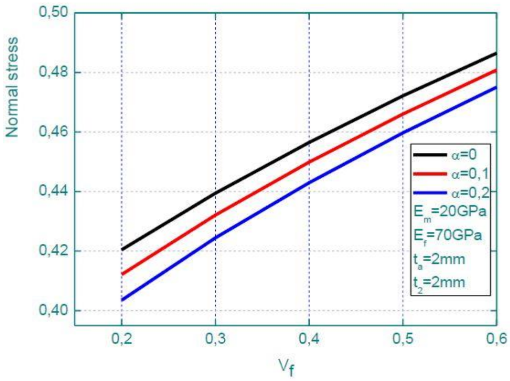

(b) Glass FRP

Fig. 10 Porosity effect as function of fibers volume fraction on normal stress of RC beam strengthened with Kevlar and Glass FRP plate

Figs. 8(a) and (b) show the effect of porosity versus distance from the plate end on the normal stress of a reinforced concrete beam reinforced by a Kevlar and GFRP porous composite plate, respectively. The thickness of the composite plate and adhesive is taken equal to ($t_2 = t_a = 2$ mm). It can be concluded that the porosity has a negligible effect on the normal stress as a function of the distance from the plate end.

Figs. 9(a) and (b) show the influence of the volume fraction of porosity as a function of the distance from the plate end on the shear stress of a RC beam. The volume fraction of porosity is considered equal (0, 0.1 and 0.2). In contrast to normal stress, the porosity effect as a function of distance from the plate end has a remarkable effect on shear stress. It can also be noted that the shear stresses become weaker when moving away from the plate end.

The effect of the fiber volume fraction on the normal stress of a RC beam reinforced with a porous Kevlar and GFRP composite plate is shown in Figs. 10(a) and (b), respectively. It can be seen that the porosity effect becomes lower when the reinforcing plate contains a larger volume fraction of the fibers.

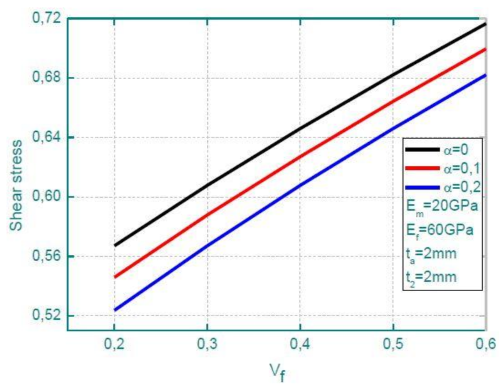

(a) Kevlar FRP

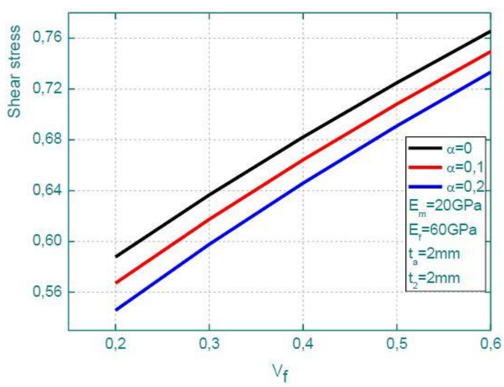

(b) Glass FRP

Fig. 11 Porosity effect as function of fibers volume fraction on shear stress of RC beam strengthened with Kevlar and Glass FRP plate

Figs. 11(a) and (b) show the influence of the volume fraction of the fibers on the shear stress of a RC beam reinforced by external bonding of the porous composite plate of Kevlar and Glass fibers, respectively. It should be noted that the shear stress becomes greater when the fiber volume fraction increases.

4. Conclusions

The effect of porosity on the interfacial stresses of a RC beam reinforced by external bonding of porous composite plates is presented in this work. The concrete beam is considered simply supported and subjected to different types of loads. The rule of mixture of the composite plate has been modified to evaluate the characteristics of the material with the porosity phases. The prediction of shear stresses and normal stresses in reinforced concrete beams by an externally bonded of porous plate provides the basis for understanding failure of concrete beams and the development of appropriate design rules. The following conclusions can be drawn from this paper:

- Based on the results of this work, the existence of pores in the reinforcement plate reduces the interface stresses. A solution can be considered for the detachment of the reinforcing plate due to the concentration of the interfacial stresses by the use of porous FRP plates especially at the end.
- The porosity effect on the interfacial stresses becomes lower as the fiber volume fraction increases in the reinforcement plate.
- Normal and shear stresses increase as the thickness of the reinforcement plate increases and decreases as the thickness of the adhesive increases.
- Interfacial stress become more important when the beam is square ($t_1/b_1 = 1$).
- Interfacial stress increase as the distance from the plate end (a) increases.

Acknowledgments

This research was supported by the Algerian Ministry of Higher Education and Scientific Research (MESRS) as part of the grant for the PRFU research project n° A01L02UN140120200002 and by the University of Tiaret, in Algeria.

References

Abdelhak, Z., Hadji, L., Khelifa, Z., Hassaine Daouadji, T. and Adda Bedia, E.A. (2016), "Analysis of buckling response of functionally graded sandwich plates using a refined shear deformation theory", *Wind Struct., Int. J.*, **22**(3), 291-305. https://doi.org/10.12989/was.2016.22.3.291

Abderezak, R., Daouadji, T.H., Abbes, B., Rabia, B., Belkacem, A. and Abbes, F. (2017), "Elastic analysis of interfacial stress concentrations in CFRP-RC hybrid beams: Effect of creep and shrinkage", *Adv. Mater. Res., Int. J.*, **6**(3), 257-278. https://doi.org/10.12989/amr.2017.6.3.257

Abderezak, R., Daouadji, T.H., Rabia, B. and Belkacem, A. (2018), "Nonlinear analysis of damaged RC beams strengthened with glass fiber reinforced polymer plate under symmetric loads", *Earthq. Struct., Int. J.*, **15**(2), 113-122. https://doi.org/10.12989/eas.2018.15.2.113

Abderezak, R., Rabia, B., Daouadji, T.H., Abbes, B., Belkacem, A. and Abbes, F. (2019), "Elastic analysis of interfacial stresses in prestressed PFGM-RC hybrid beams", *Adv. Mater. Res., Int. J.*, **7**(2), 83-103. https://doi.org/10.12989/amr.2018.7.2.083

Abderezak, R., Daouadji, T.H. and Rabia, B. (2020), “Analysis of interfacial stresses of the reinforced concrete foundation beams repairing with composite materials plate”, *Coupl. Syst. Mech., Int. J.*, **9**(5), 473-498. http://doi.org/10.12989/csm.2020.9.5.473

Abualnour, M., Chikh, A., Hebali, H., Kaci, A., Tounsi, A., Bousahla, A.A. and Tounsi, A. (2019), “Thermomechanical analysis of antisymmetric laminated reinforced composite plates using a four variable trigonometric refined plate theory”, *Comput. Concrete, Int. J.*, **24**(6), 489-498. https://doi.org/10.12989/cac.2019.24.6.489

Addou, F.Y., Meradjah, M., Bousahla, A.A., Benachour, A., Bourada, F., Tounsi, A. and Mahmoud, S.R. (2019), “Influences of porosity on dynamic response of FG plates resting on Winkler/Pasternak/Kerr foundation using quasi 3D HSDT”, *Comput. Concrete, Int. J.*, **24**(4), 347-367. https://doi.org/10.12989/cac.2019.24.4.347

Adim, B. and Daouadji, T.H. (2016), “Effects of thickness stretching in FGM plates using a quasi-3D higher order shear deformation theory”, *Adv. Mater. Res., Int. J.*, **5**(4), 223-244. https://doi.org/10.12989/amr.2016.5.4.223

Ahmed, E., Sobuz, H.R. and Sutan, N.M. (2011), “Flexural performance of CFRP strengthened RC beams with different degrees of strengthening schemes”, *Int. J. Phys. Sci.*, **6**(9), 2229-2238. https://doi.org/10.5897/IJPS11.304

Al-Furjan, M.S.H., Safarpour, H., Habibi, M., Safarpour, M. and Tounsi, A. (2020), “A comprehensive computational approach for nonlinear thermal instability of the electrically FG-GPLRC disk based on GDQ method”, *Eng. Comput.*, 1-18. https://doi.org/10.1007/s00366-020-01088-7

Alam, M.A. and Al Riyami, K. (2018), “Shear strengthening of reinforced concrete beam using natural fibre reinforced polymer laminates”, *Constr. Build. Mater.*, **162**(20), 683-696. https://doi.org/10.1016/j.conbuildmat.2017.12.011

Alimirzaei, S., Mohammadimehr, M. and Tounsi, A. (2019), “Nonlinear analysis of viscoelastic micro-composite beam with geometrical imperfection using FEM: MSGT electro-magneto-elastic bending, buckling and vibration solutions”, *Struct. Eng. Mech., Int. J.*, **71**(5), 485-502. https://doi.org/10.12989/sem.2019.71.5.485

Arani, A.G., Khoddami Maraghi, Z., Khani, M. and Alinaghian, I. (2017), “Free vibration of embedded porous plate using third-order shear deformation and poroelasticity theories”, *J. Eng.*, 2017. https://doi.org/10.1155/2017/1474916

Ashour, A.F., El-Refaie, S.A. and Garrity, S.W. (2004), “Flexural strengthening of RC continuous beams using CFRP laminates”, *Cement Concrete Compos.*, **26**, 765-775. https://doi.org/10.1016/j.cemconcomp.2003.07.002

Balubaid, M., Tounsi, A., Dakhel, B. and Mahmoud, S.R. (2019), “Free vibration investigation of FG nanoscale plate using nonlocal two variables integral refined plate theory”, *Comput. Concrete, Int. J.*, **24**(6), 579-586. https://doi.org/10.12989/cac.2019.24.6.579

Batou, B., Nebab, M., Bennai, R., Atmane, H.A., Tounsi, A. and Bouremana, M. (2019), “Wave dispersion properties in imperfect sigmoid plates using various HSDTs”, *Steel Compos. Struct., Int. J.*, **33**(5), 699-716. https://doi.org/10.12989/scs.2019.33.5.699

Belbachir, N., Draich, K., Bousahla, A.A., Bourada, M., Tounsi, A. and Mohammadimehr, M. (2019), “Bending analysis of anti-symmetric cross-ply laminated plates under nonlinear thermal and mechanical loadings”, *Steel Compos. Struct., Int. J.*, **33**(1), 81-92. https://doi.org/10.12989/scs.2019.33.1.081

Belbachir, N., Bourada, M., Draiche, K., Tounsi, A., Bourada, F., Bousahla, A.A. and Mahmoud, S.R (2020), “Thermal flexural analysis of anti-symmetric cross-ply laminated plates using a four variable refined theory”, *Smart Struct. Syst., Int. J.*, **25**(4), 409-422. https://doi.org/10.12989/sss.2020.25.4.409

Belkacem, A., Tahar, H.D., Abderrezak, R., Amine, B.M., Mohamed, Z. and Boussad, A. (2018), “Mechanical buckling analysis of hybrid laminated composite plates under different boundary conditions”, *Struct. Eng. Mech., Int. J.*, **66**(6), 761-769. https://doi.org/10.12989/sem.2018.66.6.761

Benferhat, R., Hassaine Daouadji. T., Said Mansour, M and Hadji L. (2016a), “Effect of porosity on the bending and free vibration response of functionally graded plates resting on Winkler-Pasternak foundations”, *Earthq. Struct., Int. J.*, **10**(6) ,1429-1449. https://doi.org/10.12989/eas.2016.10.6.1429

Benferhat, R., Hassaine Daouadji, T., Hadji, L. and Said Mansour, M. (2016b), "Static analysis of the FGM plate with porosities", *Steel Compos. Struct., Int. J.*, **21**(1), 123-136. https://doi.org/10.12989/scs.2016.21.1.123
Benhenni, M.A., Daouadji, T.H., Abbes, B., Adim, B., Li, Y. and Abbes, F. (2018), "Dynamic analysis for anti-symmetric cross-ply and angle-ply laminates for simply supported thick hybrid rectangular plates", *Adv. Mater. Res., Int. J.*, **7**(2), 83-103. https://doi.org/10.12989/amr.2018.7.2.119
Benhenni, M.A., Daouadji, T.H., Abbes, B., Abbes, F., Li, Y. and Adim, B. (2019a), "Numerical analysis for free vibration of hybrid laminated composite plates for different boundary conditions", *Struct. Eng. Mech., Int. J.*, **70**(5), 535-549. https://doi.org/10.12989/sem.2019.70.5.535
Benhenni, M.A., Adim, B., Daouadji, T.H., Abbès, B., Abbès, F., Li, Y. and Bouzidane, A. (2019b), "A comparison of closed form and finite element solutions for the free vibration of hybrid cross ply laminated plates", *Mech. Compos. Mater.*, **55**(2),181-194. https://doi.org/10.1007/s11029-019-09803-2
Bensattalah, T., Daouadji, T.H., Zidour, M., Tounsi, A. and Bedia, E.A. (2016), "Investigation of thermal and chirality effects on vibration of single walled carbon nanotubes embedded in a polymeric matrix using nonlocal elasticity theories", *Mech. Compos. Mater.*, **52**(4), 555-568. https://doi.org/10.1007/s11029-016-9606-z
Bensattalah, T., Zidour, M. and Daouadji, T.H. (2018), "Analytical analysis for the forced vibration of CNT surrounding elastic medium including thermal effect using nonlocal Euler-Bernoulli theory", *Adv. Mater. Res., Int. J.*, **7**(3), 163-174. https://doi.org/10.12989/amr.2018.7.3.163
Berghouti, H., Adda Bedia, E.A., Benkhedda, A. and Tounsi, A. (2019), "Vibration analysis of nonlocal porous nanobeams made of functionally graded material", *Adv. Nano Res., Int. J.*, **7**(5), 351-364. https://doi.org/10.12989/anr.2019.7.5.351
Bouakaz, K., Daouadji, T.H., Meftah, S.A., Ameur, M., Tounsi, A. and Bedia, E.A. (2014), "A numerical analysis of steel beams strengthened with composite materials", *Mech. Compos. Mater.*, **50**(4), 685-696. https://doi.org/10.1007/s11029-014-9435-x
Bourada, F., Bousahla, A.A., Bourada, M., Azzaz, A., Zinata, A. and Tounsi, A. (2019), "Dynamic investigation of porous functionally graded beam using a sinusoidal shear deformation theory", *Wind Struct., Int. J.*, **28**(1), 19-30. https://doi.org/10.12989/was.2019.28.1.019
Bourada, F., Bousahla, A.A., Tounsi, A., Bedia, E.A., Mahmoud, S.R., Benrahou, K.H. and Tounsi, A. (2020), "Stability and dynamic analyses of SW-CNT reinforced concrete beam resting on elastic-foundation", *Comput. Concrete, Int. J.*, **25**(6), 485-495. https://doi.org/10.12989/cac.2020.25.6.485
Bousahla, A.A., Bourada, F., Mahmoud, S.R., Tounsi, A., Algarni, A., Bedia, E.A. and Tounsi, A. (2020), "Buckling and dynamic behavior of the simply supported CNT-RC beams using an integral-first shear deformation theory", *Comput. Concrete, Int. J.*, **25**(2), 155-166. https://doi.org/10.12989/cac.2020.25.2.155
Boussoula, A., Boucham, B., Bourada, M., Bourada, F., Tounsi, A., Bousahla, A.A. and Tounsi, A. (2020), "A simple nth-order shear deformation theory for thermomechanical bending analysis of different configurations of FG sandwich plates", *Smart Struct. Syst., Int. J.*, **25**(2), 197-218. https://doi.org/10.12989/sss.2020.25.2.197
Boutaleb, S., Benrahou, K.H., Bakora, A., Algarni, A., Bousahla, A.A., Tounsi, A., Tounsi, A. and Mahmoud, S.R. (2019), "Dynamic Analysis of nanosize FG rectangular plates based on simple nonlocal quasi 3D HSDT", *Adv. Nano Res., Int. J.*, **7**(3), 191-208. https://doi.org/10.12989/anr.2019.7.3.191
Chedad, A., Daouadji, T.H., Abderezak, R., Belkacem, A., Abbes, B., Rabia, B. and Abbes, F. (2017), "A high-order closed-form solution for interfacial stresses in externally sandwich FGM plated RC beams", *Adv. Mater. Res., Int. J.*, **6**(4) 317-328. https://doi.org/10.12989/amr.2017.6.4.317
Chedad, A., Daouadji, T.H., Abderezak, R., Belkacem, A., Abbes, B., Rabia, B. and Abbes, F. (2018), "A high-order closed-form solution for interfacial stresses in externally sandwich FGM plated RC beams", *Adv. Mater. Res., Int. J.*, **6**(4), 317-328. https://doi.org/10.12989/amr.2017.6.4.317
Chergui, S., Daouadji, T.H., Hamrat, M., Boulekbache, B., Bougara, A., Abbes, B. and Amziane, S. (2019), "Interfacial stresses in damaged RC beams strengthened by externally bonded prestressed GFRP laminate plate: Analytical and numerical study", *Adv. Mater. Res., Int. J.*, **8**(3), 197-217. https://doi.org/10.12989/amr.2019.8.3.197

Chikr, S.C., Kaci, A., Bousahla, A.A., Bourada, F., Tounsi, A., Bedia, E.A., Mahmoud, S.R., Benrahou, K.H. and Tounsi, A. (2019), "Analytical study of bending and free vibration responses of functionally graded beams resting on elastic foundation", *Struct. Eng. Mech., Int. J.*, **71**(2), 185-196. https://doi.org/10.12989/sem.2019.71.2.185

Chikr, S.C., Kaci, A., Bousahla, A.A., Bourada, F., Tounsi, A., Bedia, E.A., Mahmoud, S.R., Benrahou, K.H. and Tounsi, A. (2020), "A novel four-unknown integral model for buckling response of FG sandwich plates resting on elastic foundations under various boundary conditions using Galerkin's approach", *Geomech. Eng., Int. J.*, **21**(5), 471-487. https://doi.org/10.12989/gae.2020.21.5.471

Daouadji, T.H. (2013), "Analytical analysis of the interfacial stress in damaged reinforced concrete beams strengthened by bonded composite plates", *Strength Mater.*, **45**(5), 587-597. htttps://doi.org/10.1007/s11223-013-9496-4

Daouadji, T.H. (2016), "Theoretical analysis of composite beams under uniformly distributed load", *Adv. Mater. Res., Int. J.*, **5**(1), 1-9. https://doi.org/10.12989/amr.2016.5.1.001

Daouadji, T.H. (2017), "Analytical and numerical modeling of interfacial stresses in beams bonded with a thin plate", *Adv. Computat. Des., Int. J.*, **2**(1), 57-69. https://doi.org/10.12989/acd.2017.2.1.057

Daouadji, T.H. and Adim, B. (2016), "An analytical approach for buckling of functionally graded plates", *Adv. Mater. Res., Int. J.*, **5**(3), 141-169. https://doi.org/10.12989/amr.2016.5.3.141

Daouadji, T.H. and Benferhat, R. (2016), "Bending analysis of an imperfect FGM plates under hygro-thermo-mechanical loading with analytical validation", *Adv. Mater. Res., Int. J.*, **5**(1), 35-53. https://doi.org/10.12989/amr.2016.5.1.035

Daouadji, T.H., Rabahi, A., Abbes, B. and Adim, B. (2016), "Theoretical and finite element studies of interfacial stresses in reinforced concrete beams strengthened by externally FRP laminates plate", *J. Adhes. Sci. Technol.*, **30**(12), 1253-1280. https://doi.org/10.1080/01694243.2016.1140703

Daouadji, T.H., Boussad, A., Abderezak, R., Rabia, B., Fazilay, A. and Belkacem, A. (2019), "Flexural behaviour of steel beams reinforced by carbon fibre reinforced polymer: Experimental and numerical study", *Struct. Eng. Mech., Int. J.*, **72**(4), 409-419. https://doi.org/10.12989/sem.2019.72.4.409

Daouadji, T.H., Abderezak, R. and Rabia, B. (2020), "Flexural performance of wooden beams strengthened by composite plate", *Struct. Monitor. Maint., Int. J.*, **7**(3), 233-259. http://doi.org/10.12989/smm.2020.7.3.233

De Lorenzis, L. and Zavarise, G. (2009), "Cohesive zone modeling of interfacial stresses in plated beams", *Int. J. Solids Struct.*, **46**, 4181-4191. https://doi.org/10.1061/(asce)0899-1561(1997)9:4(206)

Draiche, K., Bousahla, A.A., Tounsi, A., Alwabli, A.S., Tounsi, A. and Mahmoud, S.R. (2019), "Static analysis of laminated reinforced composite plates using a simple first-order shear deformation theory", *Comput. Concrete, Int. J.*, **24**(4), 369-378. https://doi.org/10.12989/cac.2019.24.4.369

Du, Y., Liu, Y. and Zhou, F. (2019), "An improved four-parameter model on stress analysis of adhesive layer in plated beam", *Int. J. Adhes. Adhes.*, **91**, 1-11. https://doi.org/10.1016/j.ijadhadh.2019.02.005

Esfahani, M.R., Kianoush, M.R. and Tajari, A.R. (2007), "Flexural behaviour of reinforced concrete beams strengthened by CFRP sheets", *Eng. Struct.*, **29**(10), 2428-2444. https://doi.org/10.1016/j.engstruct.2006.12.008

Gao, P., Gu, X. and Mosallam, A.S. (2016), "Flexural behavior of preloaded reinforced concrete beams strengthened by prestressed CFRP laminates", *Compos. Struct.*, **157**(1), 33-50. https://doi.org/10.1016/j.compstruct.2016.08.013

Ghafoori, E., Hosseini, A., Al-Mahaidi, R., Zhao, X.L. and Motavalli, M. (2018), "Prestressed CFR- P-strengthening and long-term wireless monitoring of an old roadway metallic bridge", *Eng. Struct.*, **176**, 585-605. https://doi.org/10.1016/j.engstruct.2018.09.042

Hadji, L., Daouadji, T.H., Meziane, M. and Bedia, E.A. (2016), "Analyze of the interfacial stress in reinforced concrete beams strengthened with externally bonded CFRP plate", *Steel Compos. Struct., Int. J.*, **20**(2), 413-429. https://doi.org/10.12989/scs.2016.20.2.413

Hadj, B., Rabia, B. and Daouadji, T.H. (2019), "Influence of the distribution shape of porosity on the bending FGM new plate model resting on elastic foundations", *Struct. Eng. Mech., Int. J.*, **72**(1), 823-832. https://doi.org/10.12989/sem.2019.72.1.061

Hamrat, M., Bouziadi, F., Boulekbache, B., Daouadji, T.H., Chergui, S., Labed, A. and Amziane, S. (2020), "Experimental and numerical investigation on the deflection behavior of pre-cracked and repaired reinforced concrete beams with fiber-reinforced polymer", *Constr. Build. Mater.*, **249**, 118745. https://doi.org/10.1016/j.conbuildmat.2020.118745

Hao, S.W., Liu, Y. and Liu, X.D. (2012), "Improved interfacial stress analysis of a plated beam", *Struct. Eng. Mech., Int. J.*, **44**(6), 815-837. https://doi.org/10.12989/sem.2012.44.6.815

Hojatkashani, A. and Kabir, M.Z. (2012), "Interfacial stress assessment at the cracked zones in CFRP retrofitted RC beams", *Struct. Eng. Mech., Int. J.*, **44**(6), 705-733. https://doi.org/10.12989/sem.2012.44.6.705

Hosseini, A., Ghafoori, E., Al-Mahaidi, R., Zhao, X.L. and Motavalli, M. (2019), "Strengthening of a 19th-century roadway metallic bridge using nonprestressed bonded and prestressed unbonded CFRP plates", *Constr. Build. Mater.*, **209**, 240-259. https://doi.org/10.1016/j.conbuildmat.2019.03.095

Hussain, M., Naeem, M.N., Khan, M.S. and Tounsi, A. (2020), "Computer-aided approach for modelling of FG cylindrical shell sandwich with ring supports", *Comput. Concrete, Int. J.*, **25**(5), 411-425. https://doi.org/10.12989/cac.2020.25.5.411

Kaddari, M., Kaci, A., Bousahla, A.A., Tounsi, A., Bourada, F., Tounsi, A., Bedia, E.A. and Al-Osta, M.A. (2020), "A study on the structural behaviour of functionally graded porous plates on elastic foundation using a new quasi-3D model: Bending and Free vibration analysis", *Comput. Concrete, Int. J.*, **25**(1), 37-57. https://doi.org/10.12989/cac.2020.25.1.037

Karami, B., Janghorban, M. and Tounsi, A. (2019), "Galerkin's approach for buckling analysis of functionally graded anisotropic nanoplates/different boundary conditions", *Eng. Comput.*, **35**, 1297-1316. https://doi.org/10.1007/s00366-018-0664-9

Khan, U., Al-Osta, M.A. and Ibrahim, A. (2017), "Modeling shear behavior of reinforced concrete beams strengthened with externally bonded CFRP sheets", *Struct. Eng. Mech., Int. J.*, **61**(1), 125-142. https://doi.org/10.12989/sem.2017.61.1.125

Khiloun, M., Bousahla, A.A., Kaci, A., Bessaim, A., Tounsi, A. and Mahmoud, S.R. (2020), "Analytical modeling of bending and vibration of thick advanced composite plates using a four-variable quasi 3D HSDT", *Eng. Comput.*, **36**(3), 807-821. https://doi.org/10.1007/s00366-019-00732-1

Liang, J.F., Yu, D., Xie, S. and Li, J. (2017), "Flexural behaviour of reinforced concrete beams strengthened with NSM CFRP prestressed prisms", *Struct. Eng. Mech., Int. J.*, **62**(3), 291-295. https://doi.org/10.12989/sem.2017.62.3.297

Matouk, H., Bousahla, A.A., Heireche, H., Bourada, F., Bedia, E.A., Tounsi, A., Mahmoud, S.R., Tounsi, A. and Benrahou, K.H. (2020), "Investigation on hygro-thermal vibration of P-FG and symmetric S-FG nanobeam using integral Timoshenko beam theory", *Adv. Nano Res., Int. J.*, **8**(4), 293-305. https://doi.org/10.12989/anr.2020.8.4.293

Medani, M., Benahmed, A., Zidour, M., Heireche, H., Tounsi, A., Bousahla, A.A., Tounsi, A. and Mahmoud, S.R. (2019), "Static and dynamic behavior of (FG-CNT) reinforced porous sandwich plate using energy principle", *Steel Compos. Struct., Int. J.*, **32**(5), 595-610. https://doi.org/10.12989/scs.2019.32.5.595

Mohammed, A.A., Manalo, A.C., Ferdous, W., Zhuge, Y., Vijay, P.V., Alkinani, A.Q. and Fam, A. (2020), "State-of-the-art of prefabricated FRP composite jackets for structural repair", *Eng. Sci. Technol., Int. J.*, **23**(5), 1244-1258. https://doi.org/10.1016/j.jestch.2020.02.006

Narayanamurthy, V., Chen, J.F., Cairns, J. and Ramaswamy, A. (2011), "Effect of shear deformation on interfacial stresses in plated beams subjected to arbitrary loading", *Int. J. Adhes. Adhes.*, **31**(8), 862-874. https://doi.org/10.1016/j.ijadhadh.2011.08.007

Rabahi, A., Daouadji, T.H., Abbes, B. and Adim, B. (2016), "Analytical and numerical solution of the interfacial stress in reinforced-concrete beams reinforced with bonded prestressed composite plate", *J. Reinf. Plast. Compos*, **35**(3), 258-272. https://doi.org/10.1177/0731684415613633

Rabhi, M., Benrahou, K.H., Kaci, A., Houari, M.S.A., Bourada, F., Bousahla, A.A., Tounsi, A., Adda Bedia, E.A., Mahmoud, S.R. and Tounsi, A. (2020), "A new innovative 3-unknowns HSDT for buckling and free vibration of exponentially graded sandwich plates resting on elastic foundations under various boundary conditions", *Geomech. Eng., Int. J.*, **22**(2), 119-132. http://doi.org/10.12989/gae.2020.22.2.119

Rabia, B., Abderezak, R., Daouadji, T.H., Abbes, B., Belkacem, A. and Abbes, F. (2018), "Analytical analysis of the interfacial shear stress in RC beams strengthened with prestressed exponentially-varying properties plate", *Adv. Mater. Res., Int. J.*, **7**(1), 29-44. https://doi.org/10.12989/amr.2018.7.1.029

Rabia, B., Daouadji, T.H. and Abderezak, R. (2019a), "Effect of porosity in interfacial stress analysis of perfect FGM beams reinforced with a porous functionally graded materials plate", *Struct. Eng. Mech., Int. J.*, **72**(3), 293-304. https://doi.org/10.12989/sem.2019.72.3.293

Rabia, B., Daouadji, T.H. and Abderezak, R. (2019b), "Effect of distribution shape of the porosity on the interfacial stresses of the FGM beam strengthened with FRP plate", *Earthq. Struct., Int. J.*, **16**(5), 601-609. https://doi.org/10.12989/eas.2019.16.5.601

Rahmani, M.C., Kaci, A., Bousahla, A.A., Bourada, F., Tounsi, A., Bedia, E.A., Mahmoud, S.R., Benrahou, K.H. and Tounsi, A. (2020), "Influence of boundary conditions on the bending and free vibration behavior of FGM sandwich plates using a four-unknown refined integral plate theory", *Comput. Concrete, Int. J.*, **25**(3), 225-244. https://doi.org/10.12989/cac.2020.25.3.225

Refrafi, S., Bousahla, A.A., Bouhadra, A., Menasria, A., Bourada, F., Tounsi, A., Bedia, E.A., Mahmoud, S.R., Benrahou, K.H. and Tounsi, A. (2020), "Effects of hygro-thermo-mechanical conditions on the buckling of FG sandwich plates resting on elastic foundations", *Comput. Concrete, Int. J.*, **25**(4), 311-325. https://doi.org/10.12989/cac.2020.25.4.311

Sahla, M., Saidi, H., Draiche, K., Bousahla, A.A., Bourada, F. and Tounsi, A. (2019), "Free vibration analysis of angle-ply laminated composite and soft core sandwich plates", *Steel Compos. Struct., Int. J.*, **33**(5), 663-679. https://doi.org/10.12989/scs.2019.33.5.663

Shariati, A., Ghabussi, A., Habibi, M., Safarpour, H., Safarpour, M., Tounsi, A. and Safa, M. (2020), "Extremely large oscillation and nonlinear frequency of a multi-scale hybrid disk resting on nonlinear elastic foundations", *Thin-Wall. Struct*, **154**, 106840. https://doi.org/10.1016/j.tws.2020.106840

Shen, H.S., Teng, J.G. and Yang, J. (2001), "Interfacial stresses in beams and slabs bonded with thin plate", *J. Eng. Mech.*, **127**(4), 339-406. https://doi.org/10.1061/(ASCE)0733-9399(2001)127:4(399)

Siddika, A., Al Mamun, M.A., Alyousef, R. and Amran, Y.M. (2019), "Strengthening of reinforced concrete beams by using fiber-reinforced polymer composites: A review", *J. Build. Eng.*, **25**, 100798. https://doi.org/10.1016/j.jobe.2019.100798

Siddika, A., Al Mamun, M.A., Ferdous, W. and Alyousef, R. (2020), "Performances, challenges and opportunities in strengthening reinforced concrete structures by using FRPs-A state-of-the-art review", *Eng. Fail. Anal.*, **111**, 104480. https://doi.org/10.1016/j.engfailanal.2020.104480

Smith, S.T. and Teng, J.G. (2001), "Interfacial stresses in plated beams", *Eng. Struct.*, **23**(7), 857-871. http://doi.org/10.1016/S0141-0296(00)00090-0

Täljsten, B. (1997), "Strengthening of beams by plate bonding", *J. Mater. Civil Eng.*, **9**(4), 206-212. https://doi.org/10.1061/(ASCE)0899-1561(1997)9:4(206)

Tayeb, B. and Daouadji, T.H. (2020), "Improved analytical solution for slip and interfacial stress in composite steel-concrete beam bonded with an adhesive", *Adv. Mater. Res., Int. J.*, **9**(2), 133-153. https://doi.org/10.12989/amr.2020.9.2.133

Teng, J.G., Zhang, J.W. and Smith, S.T. (2002), "Interfacial stresses in reinforced concrete beams bonded with a soffit plate: a finite element study", *Constr. Build. Mater.*, **16**(1), 1-14. https://doi.org/10.1016/S0950-0618(01)00029-0

Tounsi, A. (2006), "Improved theoretical solution for interfacial stresses in concrete beams strengthened with FRP plate", *Int. J. Solids Struct.*, **43**(14-15), 4154-4174. https://doi.org/10.1016/j.ijsolstr.2005.03.074

Tounsi, A., Daouadji, T.H. and Benyoucef, S. (2008), "Interfacial stresses in FRP-plated RC beams: Effect of adherend shear deformations", *Int. J. Adhes. Adhes.*, **29**, 313-351. https://doi.org/10.1016/j.ijadhadh.2008.06.008

Tounsi, A., Al-Dulaijan, S.U., Al-Osta, M.A., Chikh, A., Al-Zahrani, M.M., Sharif, A. and Tounsi, A. (2020), "A four variable trigonometric integral plate theory for hygro-thermo-mechanical bending analysis of AFG ceramic-metal plates resting on a two-parameter elastic foundation", *Steel Compos. Struct., Int. J*, **34**(4), 511-524. https://doi.org/10.12989/scs.2020.34.4.511

Triantafillou, T.C. and Deskovic, N. (1991), "Innovative prestressing with FRP sheets: mechanics of shortterm behavior", *J. Eng. Mech.*, **117**, 1652-1672. https://doi.org/10.1061/(asce)0733-9399(1991)117:7(1652)

Yang, D.S., Park, S.K. and Neale, K.W. (2009), "Flexural behaviour of reinforced concrete beams strengthened with prestressed carbon composites", *Compos. Struct.*, **88**, 497-508. https://doi.org/10.1016/j.compstruct.2008.05.016

Teng, J.G. and Yao, J. (2007), "Plate end debonding in FRP-plated RC beams — II: Strength model", *Eng. Struct.*, **29**(10), 2472-2486. https://doi.org/10.1016/j.engstruct.2006.11.023

Zangana, S., Epaarachchi, J., Ferdous, W. and Leng, J. (2020), "A novel hybridised composite sandwich core with glass, kevlar and zylon fibres–investigation under low-velocity impact", *Int. J. Impact Eng.*, **137**, 103430. https://doi.org/10.1016/j.ijimpeng.2019.103430

Zhao, X.L. and Zhang, L. (2007), "State-of-the-art review on FRP strengthened steel structures", *Eng. Struct.*, **29**(8), 1808-1823. https://doi.org/10.1016/j.engstruct.2006.10.006

Zine, A., Bousahla, A.A., Bourada, F., Benrahou, K.H., Tounsi, A., Adda Bedia, E.A., Mahmoud, S.R. and Tounsi, A. (2020), "Bending analysis of functionally graded porous plates via a refined shear deformation theory", *Comput. Concrete, Int. J.*, **26**(1), 63-74. http://doi.org/10.12989/cac.2020.26.1.063

CC